

A low-order model for moist convection

By XIANG-YU HUANG and ERLAND KÄLLÉN, *Department of Meteorology, University of Stockholm¹, Arrhenius Laboratory, S-106 91 Stockholm, Sweden*

(Manuscript received October 17, 1985; in final form January 24, 1986)

ABSTRACT

Two-dimensional, moist convection is modelled with a low-order, spectral model. Heating effects of condensation are taken into account and in particular the vertical asymmetry of the heating field is considered. Due to the interaction between the flow field and the condensational heating, hysteretic effects arise. The sensitivity of the model results to uncertain parameters like the dissipation is investigated. For an atmospherically realistic range of parameter values, it is found that the hysteretic behaviour is a robust model property.

1. Introduction

Moist convection is a very common phenomenon in the atmosphere ranging from small scale cumulus to severe thunderstorm complexes. In large-scale models of the atmosphere, these processes have to be parameterized because their scale is too small to be resolved by the models. The parameterization of these effects must be based on properties of nonhydrostatic models while most of the large-scale models rely on the hydrostatic assumption. The study of nonhydrostatic models commonly involves extensive numerical integrations (as for example in van Delden and Oerlemans, 1982 or Asai and Nakasugi, 1982). Much insight into the problem can be gained by using highly truncated, so-called 'low-order' models. Saltzman (1962) and Lorenz (1963) studied dry convection by only taking a few spectral components of the motion and temperature fields into account. These studies have been followed by many others, most of them concerned with dry convection, which is commonly known as the Rayleigh–Bénard convection problem.

When moist processes are considered, the formulation of a 'low-order' model presents some special difficulties. These are due to the complex expressions for latent heat release and the

asymmetric properties of condensation with respect to upward and downward motion. One simplified approach of the physics of condensation has been proposed by Shirer and Dutton (1979). In their model, the condensation processes have the effect of modifying the critical Rayleigh number, i.e., the critical vertical temperature gradient needed for the onset of convection. The numerical experiments of van Delden and Oerlemans (1982) show, however, that condensation processes also have several other important physical effects. One of these is the scale selection, i.e., which horizontal length scale will dominate in a particular moist convective situation. Another is a hysteretic effect, i.e., once convection has started, it will continue even if the Rayleigh number is decreased below the critical one needed for the onset of convection.

In this paper, we will develop a low-order model which will exhibit hysteretic effects, a feature not present in the low-order model of Shirer and Dutton (1979). With the low-order model we are also able to investigate parameter space and in particular to isolate the conditions under which hysteretic behaviour may be found. The moist convective problem is investigated using a two-dimensional Boussinesq model. The effect of moisture is only introduced via condensational heating. The condensed water is assumed to rain out instantly and thus no evaporative

¹ Contribution no. 542.

cooling will result. We expand the motion and temperature fields in spectral components and obtain a low-order model by considering a few of these components. The non-linearities retained in the low-order model are of two different kinds. One is due to advection of heat by the motion field while the other is due to the nonlinear effects of the condensational heating. The model will be formulated in Section 2 and the low-order spectral representation of the model will be developed in Section 3. Equilibrium states and stability studies will be presented in Section 4 along with a parameter sensitivity analysis. The conclusions are finally given in Section 5.

2. The model

In this section, we will develop the model. The central theme is to model the condensation process and to simplify it by successive approximations. Finally a non-dimensional scaling procedure is applied.

2.1. The basic equations

We consider two-dimensional flow between two horizontal boundaries which are assumed to have an infinite heat capacity. We thus keep the temperatures at the top and bottom constant (see Fig. 1). In a state of rest, we have the temperature distribution $T_0(z)$. When convection has begun, the temperature deviation from $T_0(z)$ is given by θ .

As basic equations we choose the Boussinesq approximated vorticity equation and the thermodynamic equation in a two-dimensional (y, z) plane (Lorenz, 1963):

$$\frac{\partial \nabla^2 \Psi}{\partial t} = -\frac{\partial(\Psi, \nabla^2 \Psi)}{\partial(y, z)} + g\alpha \frac{\partial \theta}{\partial y} + \nu \nabla^4 \Psi, \tag{2.1}$$

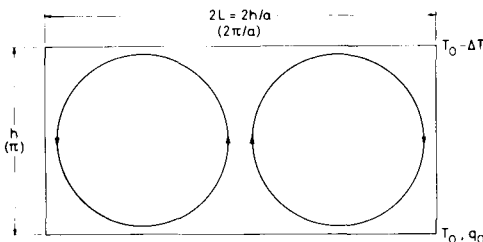


Fig. 1. The structure of fluid motion and boundary conditions.

$$\frac{\partial \theta}{\partial t} = -\frac{\partial(\Psi, \theta)}{\partial(y, z)} + S \frac{\partial \Psi}{\partial y} + \kappa \nabla^2 \theta + Q. \tag{2.2}$$

The symbols have the following meaning:

- Ψ streamfunction
- $\theta = T - T_0(z)$ temperature deviation
- g acceleration of gravity
- α coefficient of thermal expansion
- κ coefficient of thermal conductivity
- ν coefficient of kinematic viscosity
- c_p specific heat of air at constant pressure
- Q heating due to condensation
- $\Gamma = -dT_0(z)/dz$ lapse rate of $T_0(z)$
- $\Gamma_d = g/c_p$ the dry adiabatic lapse rate
- Γ_m the moist adiabatic lapse rate
- $S = \Gamma - \Gamma_d$ dry static stability
- $\partial(A, B)/\partial(y, z)$ Jacobian

The horizontal velocity v and the vertical velocity w can be calculated:

$$\begin{cases} v = -\partial \Psi / \partial z \\ w = \partial \Psi / \partial y \end{cases} \tag{2.3}$$

The lateral boundary conditions to be used are all periodic. The temperature deviation θ at the upper and lower boundaries will be kept zero. For the streamfunction Ψ , the upper and lower boundaries are taken to be free (Lorenz, 1963), in which case Ψ and $\nabla^2 \Psi$ vanish at the boundaries. The boundary conditions are:

$$\text{at } z = 0 \text{ and } z = h: \quad \Psi = \nabla^2 \Psi = \theta = 0. \tag{2.4}$$

Lateral boundary conditions:
 $\Psi, \nabla^2 \Psi$ and θ are periodic. (2.5)

The difference between (2.2) and the thermodynamic equation used by Lorenz (1963) is due to the inclusion of the condensational heating Q , and we will now turn our attention to the formulation of Q .

2.2. The heating function

To simplify the problem, we will let all condensed water rain out so that in the region of upward motion there is heating due to condensation but in the region of downward motion there

is no cooling due to evaporation. Thus the upward motion is nearly dry adiabatic below the lifting condensation level and closely follows a moist adiabat above, i.e., the rising parcels cool according to the moist adiabatic lapse rate (Γ_m). Downward motion is always close to a dry adiabat. The motion cannot be exactly adiabatic due to the inclusion of dissipative terms.

The condensational heating may be expressed as (Haltiner and Williams, 1980):

$$Q = -\frac{L_v}{c_p} \frac{dq_s}{dt} \delta_1, \tag{2.6}$$

where q_s is the saturation specific humidity, L_v is the latent heat of condensation and δ_1 is a Heaviside type of function:

$$\delta_1 = \begin{cases} 0 & w \leq 0 \quad \text{or} \quad z < z_b \\ 1 & w > 0 \quad \text{and} \quad z \geq z_b, \end{cases} \tag{2.7}$$

z_b being the height of the lifting condensation level. In the following we will assume z_b to be a constant and we will see later that z_b is one important parameter determining the nature of the moist convection.

By inserting $T = T_0(z) + \theta(y, z, t)$ and using the hydrostatic approximation and the Clausius-Clapeyron equation, (2.6) becomes:

$$-\frac{L_v}{c_p} \delta_1 \frac{dq_s}{dt} = -\frac{L_v}{c_p} \delta_1 \left[\frac{L_v}{R_d T^2} \left(\frac{d\theta}{dt} + w \frac{dT_0(z)}{dz} \right) + \frac{g}{R_d T} w \right] q_s, \tag{2.8}$$

We insert (2.8) into the thermodynamic equation (2.2), which then can be written:

$$(1 + S_q \delta_1) \frac{d\theta}{dt} = \left[S + S_q \delta_1 \left(\Gamma - \frac{gT}{\varepsilon L_v} \right) \right] w + \kappa \nabla^2 \theta, \tag{2.9}$$

where $S_q = \varepsilon L_v^2 q_s / c_p R_d T^2$. The constants used here are the gas constant of dry air R_d and the ratio of R_d and the gas constant for water vapor R_v , $\varepsilon = R_d / R_v$. It is convenient to change eq. (2.9) into the following form, which is better suited for the purpose of inserting a spectral representation

of θ :

$$\begin{aligned} d\theta/dt &= \frac{1}{1 + S_q \delta_1} \left[(1 + S_q \delta_1) S - S_q \delta_1 S \right. \\ &\quad \left. + S_q \delta_1 \Gamma - S_q \delta_1 \frac{gT}{\varepsilon L_v} \right] w + \frac{\kappa \nabla^2 \theta}{1 + S_q \delta_1} \\ &= \left[S + \frac{S_q \delta_1}{1 + S_q \delta_1} \Gamma_d \left(1 - \frac{c_p T}{\varepsilon L_v} \right) \right] w \\ &\quad + \left(1 - \frac{S_q}{1 + S_q} \delta_1 \right) \kappa \nabla^2 \theta \\ &= \left[S + \frac{\delta_1 \Gamma_d L_v q_s (\varepsilon L_v - c_p T)}{c_p R_d T^2 + \varepsilon L_v^2 q_s} \right] w \\ &\quad + (1 - \delta_1 M) \kappa \nabla^2 \theta \\ &= (S + \delta_1 H) w + (1 - \delta_1 M) \kappa \nabla^2 \theta. \end{aligned} \tag{2.10}$$

In eq. (2.10), H is a heating function coefficient which can be expressed:

$$H = \Gamma_d \frac{L_v q_s (L_v \varepsilon - c_p T)}{c_p R_d T^2 + \varepsilon L_v^2 q_s} = \Gamma_d - \Gamma_m, \tag{2.11}$$

and M is a factor modifying the dissipative term which may be written:

$$M = \frac{S_q}{1 + S_q} = \frac{\varepsilon L_v^2 q_s}{c_p R_d T^2 + \varepsilon L_v^2 q_s}. \tag{2.12}$$

The derivations of Γ_m and $\Gamma_d - \Gamma_m$ are given in Appendix A. By performing the manipulations shown in eq. (2.10), we have rescaled the thermodynamic equation. The heating function coefficient H in eq. (2.10) changes the parameter multiplying the vertical velocity from $(\Gamma - \Gamma_d)$ to $(\Gamma - \Gamma_m)$ as δ_1 changes from zero to one, i.e., as the motion changes from dry to moist convection. The factor M , which multiplies the dissipative term, originates from the factor multiplying the time derivative $d\theta/dt$ in eq. (2.9), $1 + S_q$. From eq. (2.12), we see that M is an increasing function of q_s and that $M < 1$. As the moisture content increases, the relative influence of the dissipation thus diminishes and the motion approaches a moist adiabatic process.

Besides the advection term, the thermodynamic equation as given by eq. (2.10) involves complicated nonlinearities due to H , M and δ_1 . In order to develop a low-order model, we first have to simplify the equation and we will begin by turning our attention to H and M .

One assumption is to assume a constant H and $M=0$ as in Shirer and Dutton (1979), in which case the condensational heating acts as a height independent modification to the dry static stability. However, the saturation specific humidity, q_s , decreases with height and H is therefore height dependent. Because the difference between $S = \Gamma - \Gamma_d$ on the one hand, and $H = \Gamma_d - \Gamma_m$ on the other is small, the height dependence of H may be very important.

According to its definition, the heating function coefficient, H , is not dependent on the lapse rate of the basic temperature profile if the motion is exactly moist adiabatic. In this case, T and q_s in (2.11) are determined by moist adiabatic process, i.e., H is determined only by the temperature and specific humidity at the bottom, T_0 and q_0 . However, in the real atmosphere, the upward motion cannot be exactly moist adiabatic above the lifting condensation level because of other physical processes like entrainment. Therefore, only an approximated adiabatic process can be expected.

We now assume $|\theta| < T_0(z)$ and therefore $T = T_0(z) + \theta(y, z, t)$ may be linearized around the basic state, $T_0(z)$. The saturated specific humidity q_s is then calculated using $T_0(z)$. Which temperature profile $T_0(z)$ to choose is not obvious. When condensation occurs, the basic temperature profile is modified and thus may influence H . This modification is described by the dynamical response of the model, but in this study we wish to avoid this nonlinear process by a linearization. As we are linearizing around a state of rest, we use the basic temperature profile $T_0(z) = T_0 - \Gamma z$ in the following. By just using $T_0(z)$, we systematically underestimate the temperature when evaluating H . From (2.11), the approximated heating function coefficient is expressed:

$$H(z) = \Gamma_d \frac{L_v q_s(z) (L_v \varepsilon - c_p T_0(z))}{c_p R_d T_0(z)^2 + \varepsilon L_v^2 q_s(z)}. \quad (2.13)$$

The expressions for $q_s(z)$ and the details of the derivation are given in Appendix B. Eq. (2.13) is only applied above the lifting condensation level and the specific humidity is thus always at its saturated value. In Fig. 2, three heating function coefficients are shown as functions of height, where two are linearized around $T_0(z)$ with different lapse rates and one calculated according to

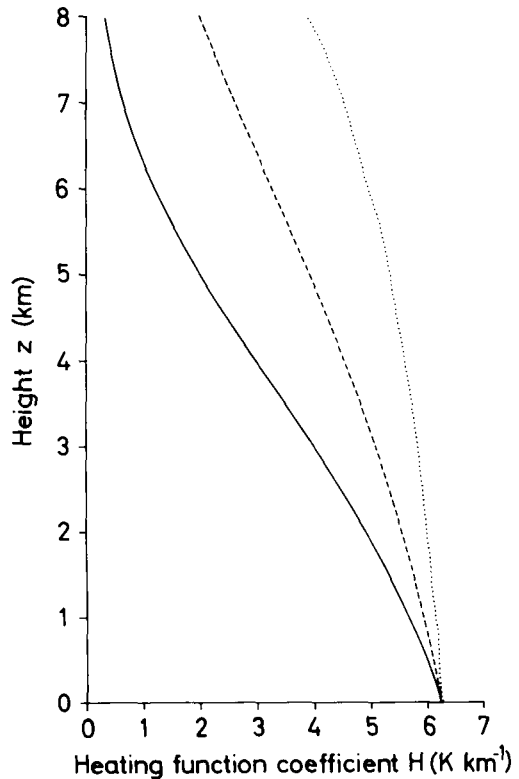


Fig. 2. The heating function coefficient $H(z)$ and $\Gamma_d - \Gamma_m$. In the figure, the full line and dashed line are heating function coefficients with lapse rates, 9.5 K km⁻¹ and 6.5 K km⁻¹ respectively. The dotted line is $\Gamma_d - \Gamma_m$. The parameters are:

$$\begin{aligned} \Gamma_d &= g/c_p = 10 \text{ K km}^{-1} \\ L_v &= 2.5 \cdot 10^6 \text{ J kg}^{-1} \\ c_p &= 1004 \text{ J kg}^{-1} \text{ K}^{-1} \\ R_d &= 287 \text{ J kg}^{-1} \text{ K}^{-1} \\ \varepsilon &= 0.622 \\ T_0(0) &= 300 \text{ K} \\ q_0(0) &= 23 \text{ g kg}^{-1} \end{aligned}$$

the moist adiabatic lapse rate. We see that the smaller the lapse rate of the basic temperature is, the larger is the heating function coefficient. We can conclude that by linearizing around the temperature $T_0(z)$, the condensational heating is underestimated, and this underestimation becomes more serious the further the actual lapse rate is removed from a moist adiabatic one.

In studies of moist convection, a more important parameter is the distribution of net heating, $(S + \delta_1 H)w$, but before we know the structure of the vertical velocity w , $(S + \delta_1 H)w$ cannot be

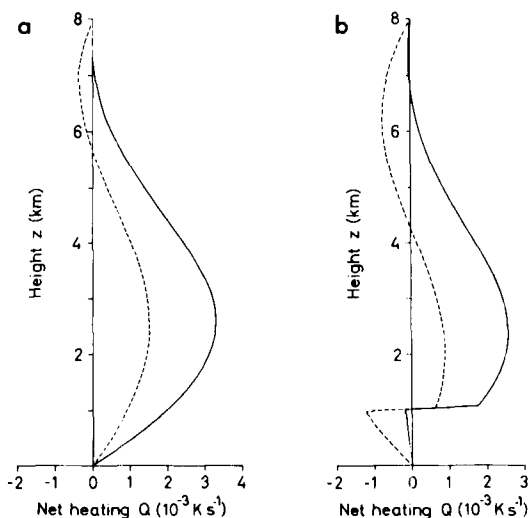


Fig. 3. The net heating due to moist adiabatic processes as a function of height z . Here we assume that the vertical velocity has a sine formed profile and W_0 is the characteristic vertical velocity. The parameters chosen to be the same as in Fig. 2 except q_0 : (a) $q_0(0) = 23 \text{ g kg}^{-1}$; (b) $q_0(0) = 15 \text{ g kg}^{-1}$.

determined. However, to get an idea of the vertical distribution of the heating, we choose a sinusoidal vertical velocity $w \sim \sin(\pi z/h)$ and then the net heating can be calculated as a function of height. In Fig. 3a and Fig. 3b, the net heating in the region of upward motion is shown with two different lapse rates of $T_0(z)$. In Fig. 3a, we choose the $T_0 = 300 \text{ K}$ and $q_0 = 23 \text{ g kg}^{-1}$ so that the height of the lifting condensation level, z_b , is practically zero. In Fig. 3b, with $T_0 = 300 \text{ K}$ and $q_0 = 15 \text{ g kg}^{-1}$, z_b is about one kilometer. From Fig. 2 and Fig. 3 we may thus conclude that condensational heating alters the effective static stability parameter from S to $(S + \delta_1 H)$ and that this effect is not evenly distributed in the vertical. The total condensational heating increases with the lapse rate of the basic temperature profile and decreases with the height of the lifting condensation level.

In the case of a vertically symmetric distribution of the vertical velocity, there will be a heating maximum at lower levels due to the vertical distribution of q_s and this will contribute to a destabilization of the atmosphere. The onset of convection will enhance the vertical motion

through a destabilization, which will further enhance condensational heating. This positive feedback is balanced by dissipation, dry adiabatic heating in the region of downward motion and the dry adiabatic cooling below z_b in the region of upward motion, which thus limit the magnitude of the motion field set up by condensation processes.

The thermodynamic dissipation coefficient is modified by a term containing the factor $\delta_1 M$ which also introduces a nonlinearity through its dependence of temperature and δ_1 . We may approximate M in the same way as H . The parameter M is then only height dependent and can be expressed:

$$M(z) = \frac{\epsilon L_v^2 q_s(z)}{c_p R_d T_0(z^2) + \epsilon L_v^2 q_s(z)} \tag{2.14}$$

In Fig. 4 we show $M(z)$ as a function of height. It is clearly seen that $M(z)$ cannot be neglected compared to the factor 1 in the eq. (2.10), especially at lower levels. As $M(z)$ decreases with height and κ is assumed to be a constant, the vertical asymmetry of the total heating profile will thus be even further enhanced.

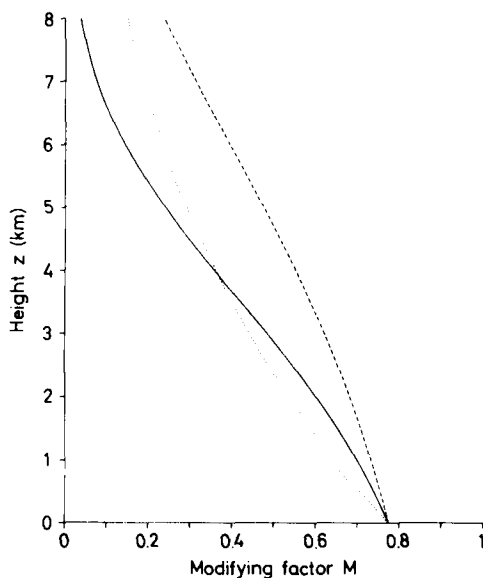


Fig. 4. The modifying factor M . In the figure, the full line and dashed line are $M(z)$ with lapse rates, 9.5 K km^{-1} and 6.5 K km^{-1} , respectively. The dotted line is M calculated from moist adiabatic values of T and q_s . The parameters are chosen to be the same as in Fig. 2.

2.3. Non-dimensional scaling

Before we proceed with further derivations, we nondimensionalize our variables as follows:

$$\begin{aligned}
 y &= \frac{h}{\pi} y' \\
 z &= \frac{h}{\pi} z' \\
 t &= \frac{h^2}{\pi^2 \kappa} t'
 \end{aligned}
 \tag{2.15}$$

$$\Psi = \kappa \Psi'$$

$$\theta = \frac{\pi^3 \kappa \nu}{g \alpha h^3} \theta'$$

Inserting (2.15) into eqs. (2.1) and (2.2), using the expressions for the condensational heating coefficient and then dropping the primes we obtain the non-dimensional equations:

$$\frac{\partial \nabla^2 \Psi}{\partial t} = - \frac{\partial(\Psi, \nabla^2 \Psi)}{\partial(y, z)} + \sigma \frac{\partial \theta}{\partial y} + \sigma \nabla^4 \Psi, \tag{2.16}$$

$$\begin{aligned}
 \frac{\partial \theta}{\partial t} &= - \frac{\partial(\Psi, \theta)}{\partial(y, z)} + (R + \delta, H_n) \frac{\partial \Psi}{\partial y} \\
 &+ (1 - \delta, M) \nabla^2 \theta.
 \end{aligned}
 \tag{2.17}$$

The boundary conditions have the same form as in (2.3) and (2.4):

$$\begin{cases}
 \Psi(y, 0) = \Psi(y, \pi) = 0 \\
 \nabla^2 \Psi(y, 0) = \nabla^2 \Psi(y, \pi) = 0 \\
 \theta(y, 0) = \theta(y, \pi) = 0
 \end{cases}
 \tag{2.18}$$

$$\begin{cases}
 \Psi(y, z) = \Psi\left(y + \frac{2\pi}{a}, z\right) \\
 \nabla^2 \Psi(y, z) = \nabla^2 \Psi\left(y + \frac{2\pi}{a}, z\right) \\
 \theta(y, z) = \theta\left(y + \frac{2\pi}{a}, z\right)
 \end{cases}
 \tag{2.19}$$

Our system has five nondimensional parameters:

- $a = h/L$ aspect ratio
- $H_n = \frac{g \alpha h^4 H(z)}{\pi^4 \nu \kappa}$ heating function coefficient
- $M_n = M(z)$ modifying factor on dissipation
- $\sigma = \nu/\kappa$ Prandtl number
- $R = \frac{g \alpha h^4 S}{\pi^4 \nu \kappa}$ Rayleigh number

In the real atmosphere, the 'dry' Rayleigh number, R , is actually negative. This is another way of saying that the mean lapse rate is statically stable under dry conditions. Our driving force for convection is the condensational heating given by $\delta, H_n w$ and $R + H_n$ must be greater than zero on the average for the atmosphere to be statically unstable under moist conditions. Due to the presence of dissipative effects $R + H_n$ must be exceed zero by a critical value which we will determine when analyzing the model properties.

Now, we have a complete set of equations with two variables, Ψ and θ , and two equations, (2.16) and (2.17). The parameters σ, a and R are constants while H_n and M_n are functions of height.

3. A low-order model for moist convection

In this section, we will develop a low-order model from eqs. (2.16) and (2.17), and then study the heating parameters in the low-order model.

We can expand Ψ and θ as Fourier series:

$$\Psi = \sum_{n=-\infty}^{\infty} \sum_{m=-\infty}^{\infty} \Psi_{nm}(t) e^{i(nay + mz)} \tag{3.1}$$

$$\theta = \sum_{n=-\infty}^{\infty} \sum_{m=-\infty}^{\infty} \theta_{nm}(t) e^{i(nay + mz)} \tag{3.2}$$

The fundamental wavelengths are $2\pi/a$ and 2π in the y and z directions, respectively. Inserting (3.1) and (3.2) into eqs. (2.16) and (2.17), a set of ordinary differential equations in the component amplitudes are obtained. Using numerical methods, it is possible to integrate these equations within any accuracy limit required, but here we choose a highly truncated model. We use one component to represent the streamfunction and three to represent the temperature deviation:

$$\begin{cases}
 \Psi = \sqrt{2} F(t) \sin ay \sin z \\
 \theta = \sqrt{2} A(t) \cos ay \sin z \\
 \quad + B(t) \sin 2z + C(t) \sin z.
 \end{cases}
 \tag{3.3}$$

The nondimensional Ψ field is plotted in Fig. 1. We will see later that the above choice of the components is the simplest one for the moist model to retain the following important properties:

- (1) the advection of the temperature deviation (through the interaction between F and A , F and B);
- (2) a horizontal change of temperature (A);
- (3) a vertical change of temperature implying a changing vertical stability (B);
- (4) a net heating or cooling (C).

By inserting (3.3) into eqs. (2.16) and (2.17), multiplying by suitable trigonometric functions, integrating from the bottom to the top and horizontally one period, we obtain the low-order model as follows:

$$\frac{dF}{dt} = -\sigma(1 + a^2)F + \frac{a\sigma}{1 + a^2} A, \tag{3.4}$$

$$\begin{aligned} \frac{dA}{dt} = & a(R + \frac{1}{2}H_a)F - (1 + a^2)(1 - \frac{1}{2}M_a)A \\ & + 4\frac{\sqrt{2}}{\pi} M_b\delta_2 B + \frac{\sqrt{2}}{\pi} \delta_2 M_a C + aFB, \end{aligned} \tag{3.5}$$

$$\begin{aligned} \frac{dB}{dt} = & a\frac{\sqrt{2}}{\pi} H_b|F| + \frac{\sqrt{2}}{\pi} (1 + a^2)M_b\delta_2 A \\ & - 4(1 - \frac{1}{2}M_c)B + \frac{1}{2}M_b C - aFA, \end{aligned} \tag{3.6}$$

$$\begin{aligned} \frac{dC}{dt} = & a\frac{\sqrt{2}}{\pi} H_a|F| + \frac{\sqrt{2}}{\pi} (1 + a^2)M_a\delta_2 A \\ & + 2M_b B - (1 - \frac{1}{2}M_a)C. \end{aligned} \tag{3.7}$$

Five constants H_a , H_b , M_a , M_b and M_c are introduced due to the condensation. They are defined as follows:

$$H_a = \frac{2}{\pi} \int_{z_b}^{\pi} H_n \sin^2 z \, dz \tag{3.8}$$

$$H_b = \frac{2}{\pi} \int_{z_b}^{\pi} H_n \sin z \sin 2z \, dz \tag{3.9}$$

$$M_a = \frac{2}{\pi} \int_{z_b}^{\pi} M_n \sin^2 z \, dz \tag{3.10}$$

$$M_b = \frac{2}{\pi} \int_{z_b}^{\pi} M_n \sin z \sin 2z \, dz \tag{3.11}$$

$$M_c = \frac{2}{\pi} \int_{z_b}^{\pi} M_n \sin^2 2z \, dz. \tag{3.12}$$

The δ_2 has the following properties:

$$\delta_2 = \begin{cases} -1 & F < 0 \\ +1 & F \geq 0, \end{cases} \tag{3.13}$$

which also brings a nonlinearity to the system in addition to the quadratic terms in the component amplitudes.

The details of the derivation of the heating integrals are given in Appendix C.

By comparing our low-order model with the same kind of low-order model for dry convection (Lorenz, 1963), it is evident that if we take away the parameters related to the condensation, i.e., let $H_a = H_b = M_a = M_b = M_c = 0$, then our model is just a Lorenz Model. The condensation adds new terms into the model and changes the coefficients of some terms. The forcing parameter of the low-order model is the Rayleigh number which is dependent mainly on the lapse rate of $T_0(z)$. The change of the forcing may be interpreted as a change of the temperature difference between upper and lower boundaries.

Condensation processes will affect the model dynamics in several ways. The most important effect is the vertical asymmetry of the heating field which is mainly determined by the lifting condensation level. In our low-order model this enters via the integration interval in determining the coefficients H_a and H_b . These parameters are seen to multiply terms including F , the stream-function amplitude, in the equations for the temperature tendencies. They are thus associated with potential energy conversion and in particular we see that they multiply terms involving the absolute value of F in eqs. (3.6) and (3.7). This is due to the assumption that condensational heating appears in the upward moving parts of the convection cell, while there is no compensating cooling in the downward moving branches. The same effect is responsible for the δ_2 multiplying the terms associated with dissipation.

A second effect of the condensational heating coefficient, which is present in eq. (3.7), is different to the first in the sense that it brings about a net heating or cooling to the whole system. The structure chosen for the temperature deviation in the A and B components does not allow a net heating of the whole domain. From physical considerations, it is however clear that the system must experience a net heating from condensation processes. We have assumed that there is an infinite supply of moisture to the system at the lower boundary and that the condensed water will rain out instantly. The net heating will in this model be described by the C -component which only has a vertical variation with a maximum at mid-level.

We have already seen that the existence of $M(z)$ favours a stronger heating at lower levels

than at upper levels and it also enhances the horizontal temperature gradient due to the properties of the δ_2 function. In other words, the condensational heating and the modifying factor on dissipation both act in the same direction in the thermodynamic process.

4. Steady-states

4.1. The equilibrium states

Before attempting to analyse the time dependent behaviour of the model defined by eqs. (3.4)–(3.7), we will first determine the steady-states and their linearized stability properties. By doing so, we obtain a good idea of the structure of the trajectory field in the four-dimensional phase-space of the low-order model.

Setting the left-hand side of eqs. (3.4)–(3.7) to zero, we see immediately that one steady-state is the trivial one where all component amplitudes are zero. Additional steady states can be found by numerical methods, but before we show results from such calculations we can investigate analytically the structure of the solutions by simplifying the equations somewhat. We first assume that $M_a = M_b = M_c = 0$, thus neglecting the effects of condensation on the dissipative terms. By doing so the steady-state equations become

$$-\sigma(1+a^2)F + \frac{a\sigma}{1+a^2}A = 0, \tag{4.1}$$

$$aR^*F - (1+a^2)A + aFB = 0, \tag{4.2}$$

$$a \frac{\sqrt{2}}{\pi} H_b |F| - 4B - aFA = 0, \tag{4.3}$$

$$\frac{\sqrt{2}}{\pi} aH_a |F| - C = 0, \tag{4.4}$$

where $R^* = R + H_a/2$ is a modified Rayleigh number. We first note that the amplitude C only appears in eq. (4.4) and from a steady-state point of view this component is decoupled from the rest of the equations. By eliminating F and B from eqs. (4.1)–(4.3) we arrive at one equation for the steady-state value of $A = A_E$ (index E indicates an equilibrium value)

$$A_E^2 - \frac{\sqrt{2}}{\pi} H_b |A_E| + \frac{4(1+a^2)^2}{a^2} (R_c - R^*) = 0, \tag{4.5}$$

where $R_c = (1+a^2)^3/a^2$. For a given value of R^* , this equation may have a maximum of four real

solutions. The elimination of F , B and C results in linear relations between F_E , B_E , C_E and A_E . Including the trivial equilibrium solutions we may thus have five steady solutions, for a given set of external parameters.

The structure of the quadratic equation (4.5) permits us to deduce under which conditions there will be one, three and five equilibrium states. If $H_b < 0$ and $R^* < R_c$ eq. (4.5) has no real solutions and we thus only have one steady-state, the trivial one of no convection. If $R^* > R_c$, eq. (4.5) has two real solutions regardless of the sign of H_b . This corresponds to states of convective motion, the two different states are simply phase reversals of the motion field (F and A change signs while B and C remain the same). If $H_b > 0$, we may finally find an interval for R^* ($R_c - [a\sqrt{2}H_b/4\pi(1+a^2)]^2 < R^* < R_c$) where five steady-states are possible. This interval lies below the critical value for the onset of convection R_c (see Lorenz, 1963), and we may thus find steady convective motion even if the forcing is below the critical one needed for onset of convection. This discussion of the steady-states may be summarized schematically as in Fig. 5 where the

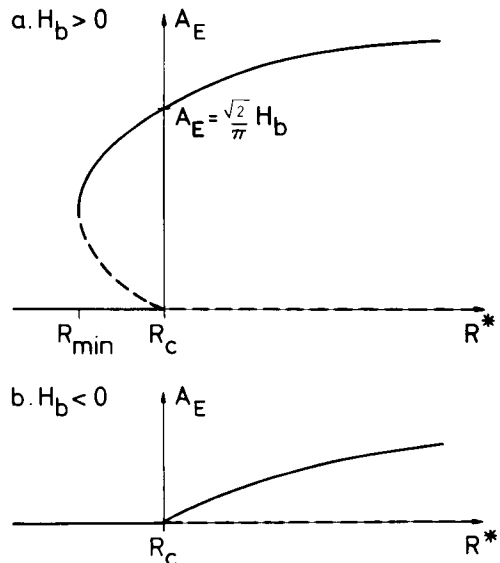


Fig. 5. Schematic figure of equilibrium state curves in two different cases, $H_b > 0$ and $H_b < 0$. We choose the Rayleigh number R as the horizontal axis and the amplitude of the first component of temperature deviation A_E as the vertical axis. The dashed parts are unstable equilibria. For further explanations, see text. (a) $H_b > 0$. (b) $H_b < 0$.

steady-state amplitude A_E is plotted as a function of R^* for the two different cases $H_b > 0$ and $H_b < 0$. For the case $H_b > 0$ we see that the steady-state branch where $A_E \neq 0$ extends below the critical value R_c . In order to determine the stability of the steady-state branches we now turn to a linearized stability analysis.

4.2. Stability study of equilibrium states

Next we determine the stability of the equilibrium states by a standard linear stability analysis. Given a small perturbation:

$$\begin{pmatrix} F \\ A \\ B \\ C \end{pmatrix} = \begin{pmatrix} F_E \\ A_E \\ B_E \\ C_E \end{pmatrix} + \begin{pmatrix} F' \\ A' \\ B' \\ C' \end{pmatrix}, \tag{4.6}$$

the linearized system can be written

$$dD/dt = ND \tag{4.7}$$

where,

$$D = \begin{pmatrix} F' \\ A' \\ B' \\ C' \end{pmatrix} \tag{4.8}$$

and

$$N = \begin{pmatrix} -\sigma(1+a^2) & \frac{a\sigma}{1+a^2} & 0 & 0 \\ a(R^* + B_E) & -(1+a^2) & aF_E & 0 \\ a\left(\frac{\sqrt{2}}{\pi} H_b \delta_2 - A_E\right) & -aF_E & -4 & 0 \\ a\frac{\sqrt{2}}{\pi} H_a \delta_2 & 0 & 0 & -1 \end{pmatrix} \tag{4.9}$$

Here, (F_E, A_E, B_E, C_E) can be any equilibrium state. The eigenvalues of the matrix N determine the stability of the equilibrium state. If any eigenvalue has a positive real part, the steady-state is unstable.

The resulting unstable equilibrium states are given in Fig. 5a by dashed lines. In the case where $H_b > 0$ (Fig. 5a) the stable steady-state curves are separated: one is along the R^* -axis for $R^* < R_c$, the others for $R^* > R_{min}$ are on either side of the R^* -axis. Between R_{min} and R_c , we have three stable equilibrium states for a given R^* . The discontinuity in the solution curve for stable equilibrium states is a remarkable feature in this

case. When $H_b < 0$ (Fig. 5b), the system has only one or two stable states to a given modified Rayleigh number R^* . When $R^* < R_c$ we have a state of rest and $R^* > R_c$ steady convection occurs. The stable equilibrium curves are continuous. We thus see that in the case where $H_b > 0$ we may obtain steady convection even if the Rayleigh number is below the critical value for the onset of convection. From a computation of H_b we have found that H_b is greater than zero if the lifting condensation level is below 2.3 km. We have also found that when z_b is below this value, the coefficients M_a , M_b and M_c are significantly different from zero. Our previous assumption of setting these coefficients to zero is thus not valid and we will have to determine the effect of these coefficients.

In the discussion above, the change of the modified Rayleigh number R^* comes from an increasing or decreasing dry static stability, S , which actually represents the change of the lapse rate of the basic state temperature, Γ . In fact, the heating parameters H_a and H_b in our low-order model are all dependent on the lapse rate of temperature which means that they cannot be kept constant when R^* changes. But we should point out that the discontinuity mentioned above is only dependent on H_b . When considering the

magnitude of the change of H_b with Γ , we have found that it is of the order $O(10^{-1} \Delta R^*)$. This effect may thus be neglected.

4.3. Steady-states of complete equations and parameter sensitivity

In our steady-state analysis we set the coefficients M_a , M_b and M_c to zero in order to simplify the algebra. It is a straightforward matter to include these coefficients into the steady-state analysis and to arrive at a quadratic equation for the equilibrium amplitude of a component. The structure of this equation is quite similar to eq. (4.5), i.e. it can be written

$$f_1 A_E^2 + f_2 |A_E| + (R_0 - R) = 0, \tag{4.10}$$

where f_1 , f_2 and R_0 depend in a complicated way on all the parameters of the problem. In this case we also find a maximum of five steady-states where one is the trivial state of no motion ($A_E = 0$). The stability properties are also similar, at the point where the trivial steady-state becomes unstable we also have the intersection between the parabolas given by eq. (4.10) and the line $A_E = 0$. An example of the equilibrium states and their stability properties is given in Fig. 6.

In our simplified steady-state analysis we found that the parameter H_b is most important for the properties of the equilibrium states. The sign of H_b determines whether there is an interval in R with five equilibrium states while the absolute value of H_b determines the width of this interval. In the complete equations the situation is not so simple, here all the integrals H_a , H_b , M_a , M_b and M_c appear in the coefficients f_1 , f_2 and

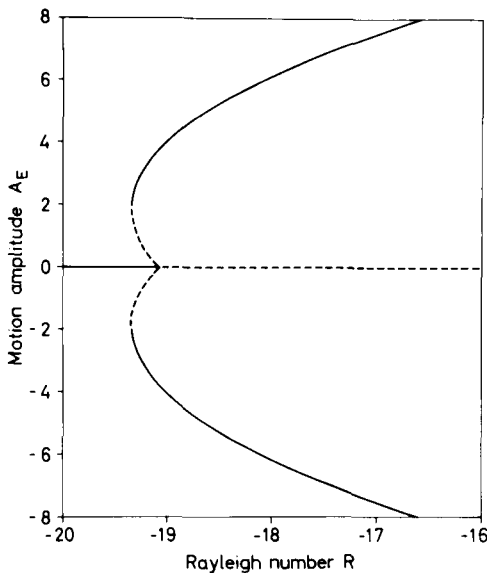


Fig. 6. Equilibrium states of the full model. Dashes indicate unstable equilibria. Motion amplitude in terms of the A -component and Rayleigh number are non-dimensional. Parameter values:
 $z_b = 1000 \text{ m}$ $T_0 = 288 \text{ K}$
 $h = 8000 \text{ m}$ $p_0 = 1.013 \cdot 10^5 \text{ Pa}$
 $a = 1$ $g = 9.8 \text{ m s}^{-2}$
 $\sigma = 1$ $\alpha = 1/300$
 $\tau = 2 \text{ hours}$ $c_p = 1004$
 $\Gamma = 5 \text{ K km}^{-1}$

R_0 of eq. (4.10). To investigate how the width of the interval with five steady-states depends on the model parameters we have to resort to numerical methods. By rewriting eq. (4.10) as

$$R = f_1(|A_E| + f_2/2f_1)^2 + R_0 - f_2^2/4f_1, \tag{4.11}$$

we see that the minimal value of $R = R_0 - f_2^2/4f_1$ is obtained when $|A_E| = -f_2/2f_1$ and when $A_E = 0$ we have $R = R_0$. The interval with five equilibrium states is thus given by $\Delta R = f_2^2/4f_1$ and it only exists when $f_1 > 0$ and $f_2 < 0$.

Furthermore we note that the critical value for the onset of convection is given by R_0 which not only depends upon the aspect ratio a (as the R_c defined earlier) but varies with all the other parameters.

We now wish to investigate how the interval ΔR and the critical value R_0 depend on some basic model parameters. The first, and perhaps most obvious, model parameter to look at is the lifting condensation level, z_b . If our results are to be interpreted as atmospherically relevant, z_b must lie within the lower parts of the atmosphere, say around 1 km. Another important and very uncertain parameter is the dissipation rate which here is given by the thermal conductivity and kinematic viscosity coefficients. By defining a Prandtl number we have fixed the ratio between these two and we need only be concerned with one of them. In the nondimensionalization procedure described in Subsection 2.3 we see from eq. (2.15) that together with the height scale the viscosity coefficients determine the non-dimensional scaling of time. In addition the viscosity coefficients enter into the non-dimensional parameters H_a , H_b and R but not into M_a , M_b and M_c . The viscosity coefficients thus determine the relative scaling between dissipative and moist adiabatic processes.

In Fig. 7, we show the critical Rayleigh number for the onset of convection as a function of the dissipation time scale τ in hours and the lifting condensation level z_b in km. The dissipation time scale is defined via the kinematic viscosity as $\tau = h^2/\pi^2\nu$ where h is the height of our model domain. The time scale τ can thus be interpreted as a relaxation time scale for entrainment processes in deep convection. It also corresponds to our nondimensional scaling of time (eq. (2.15)). The critical Rayleigh number is shown in dimensional units and thus equal to the critical

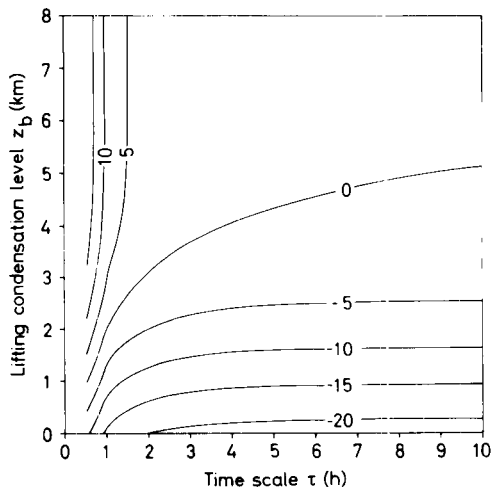


Fig. 7. Critical lapse rate for the onset of convection (S_0) in $K\ km^{-1}$ as a function of the lifting condensation level and the dissipation time scale. Parameter values same as in Fig. 6 except for z_n and τ .

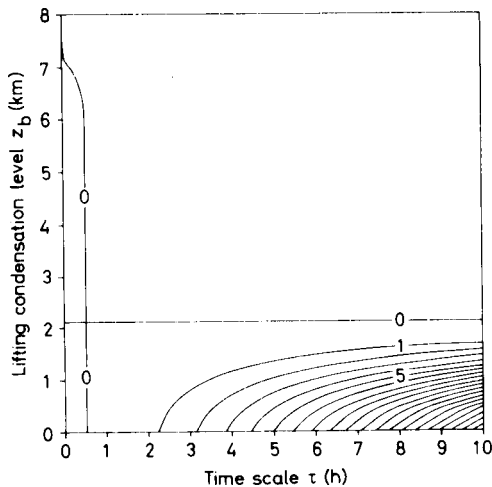


Fig. 8. Difference between the critical lapse rate needed for the onset of convection and the minimum lapse rate necessary for the maintenance of convective motion (ΔS) in $K\ km^{-1}$. Parameter values and axes same as in Fig. 7.

dry static stability, S_0 . Negative values indicate that we have onset of convection even if the flow is dry statically stable. From Fig. 7 we see that this is the case for large dissipation time scales (i.e., weak entrainment) and low lifting condensation levels. For a condensation level of 2 km and a dissipation time scale of 5 hours $S_0 = -5\ K\ km^{-1}$, i.e. the vertically imposed temperature gradient has to be greater than $\Gamma_0 + S_0 = 5\ K\ km^{-1}$ for the onset of convection. This is a very reasonable value for the atmosphere and we see from Fig. 7 that if the lifting condensation level is below 3 km, S_0 is almost independent of the dissipation time scale if it is above 3 hours. The critical value S_0 mainly depends on z_n , a behaviour very often found in the atmosphere. The independence of the dissipation time scale is reassuring as this is a very uncertain parameter in our model. In previous numerical model studies of moist convection, as for instance Asai and Nakasugi (1982), the eddy viscosity coefficient ν was chosen to be $100\ m^2\ s^{-1}$. This corresponds to a relaxation time scale of $10^5\ s$ or roughly 1 day. In the discussion of Krishnamurti (1975) an eddy viscosity of $10\ m^2\ s^{-1}$ was considered to be most realistic for atmospheric conditions and this corresponding to a time scale of around 10 days. On the other hand, observational studies indicate that the typical lifetime of a deep convection cell

does not exceed one hour (see Atkinson, 1981, pp. 331–334), while a convective storm complex may last for several hours. We therefore believe that in our simple model the dissipation time scale should be closer to an hour than to a few days, but we find it very difficult to be more precise than this. For very short dissipation time scales we need large superadiabatic lapse rates to trigger convection and the realism of these results is doubtful.

In Fig. 8, we have also plotted the interval over which convection is maintained even if the Rayleigh number is decreased below its critical value. The interval ΔS is also given in dimensional units and a direct comparison with the critical value needed for the onset of convection, S_0 can be made. We see first of all that the interval increases with an increasing dissipation time scale and a decreasing condensation level. There is a cut-off ($\Delta S = 0$) for a condensation level just above 2 km and a dissipation time scale below 0.2 hours. For realistic ranges of the dissipation time scale and the lifting condensation level we thus have a non-zero ΔS and we find that once convection has started it can persist even if the Rayleigh number is decreased below its critical value. The interval ΔS is reasonable for atmospheric conditions, it ranges from 0 to about 10 K

km^{-1} as can be seen in Fig. 8. We should remark that the dimensional values of S_0 and ΔS are very sensitive to the choice of h , the depth scale of convection. This parameter enters to the power of four in the expression for the Rayleigh number, and small changes in h will thus give large changes in S for a given R .

We have also investigated the dependence of ΔS on the aspect ratio, a , and the Prandtl number, σ . The dependence is generally weak for variations within a factor of two and we consistently find that the most important model parameter is the lifting condensation level, z_h . This indicates a robustness of the model properties to variations in parameter values and in particular we are able to conclude that uncertain parameter values like the dissipation time scale are not crucial for the model properties as long as they lie within a realistic range.

5. Conclusions

In the present study a low-order model is analyzed to examine the effect of moisture in convection. The condensed water is assumed to rain out immediately so that no cooling due to evaporation occurs. We assume a Boussinesq approximated model. The effect of condensation is included as a heating term in the thermodynamic equation. Further approximations are made with regard to the heating function in order to simplify the model formulation.

With the very simplest formulation of the moist low-order model, we are able to determine the model properties analytically. We find an instability occurring at a critical value of the imposed temperature difference between the horizontal boundaries. This instability is very similar to the one found in the dry convection problem (Lorenz, 1963), except that here the numerical value is modified by the presence of moisture. This effect has also been demonstrated by Shirer and Dutton (1979). In addition we also find an extra backbending of the equilibrium curve, which implies hysteretic behaviour in a time dependent integration. This effect arises due to the release of latent heat when convection has been initiated. Provided that there is a vertical asymmetry of this latent heat release, the latent heat will act to increase the vertical temperature gradient and thus to enhance the convection. The

asymptotic intensity of the convection is determined by the dissipative processes included in the model. These dissipative processes act to simulate the entrainment process in the atmosphere.

In a parameter sensitivity analysis, we find that the most crucial parameter in the model is the lifting condensation level. This level is also a measure of the amount of latent heat which is released in the model and the vertical distribution of the heat release. For hysteretic effects to exist, we find that the lifting condensation level must be below about 2.3 km. The closer to the surface we find this level, the more intense the hysteretic behaviour becomes. The model sensitivity to other parameters such as the dissipation time scale and the aspect ratio is not so marked. As long as the dissipation is sufficiently weak, with a relaxation time above 2 hours, the qualitative behaviour of the model is relatively unchanged. The aspect ratio, which in previous work has been considered to be of importance for the scale selection (van Delden, 1984), has not been found to have any important impact on the model behaviour.

The hysteretic behaviour is of course not a new phenomenon in models of cumulus convection (see for example numerical simulations by van Delden and Oerlemans, 1982), but we think that we have demonstrated this phenomenon in a model which is so simple that exhaustive parameter studies easily can be done. Some investigations have found hysteretic effects in convection models without condensational heating and these are due to other physical processes not considered here. In studies by Krishnamurti (1968a,b; 1975a,b) vertical asymmetries in the horizontally averaged temperature field were found and these give rise to hysteretic behaviour and other nonlinear phenomena. In our model the same vertical asymmetry appears, but the physical origin of the heating which give rise to the asymmetry is different from Krishnamurti's. In her models turbulent heat fluxes due to changing temperatures at the horizontal boundaries and imposed vertical velocity fields are the physical origins of the asymmetric heating. In the atmosphere, these processes are also important for convection and may thus be considered as alternative explanations for hysteretic behaviour. Condensation is, however, from an energetic

point of view the most dominating process in atmospheric convection and is thus very likely to produce hysteretic effects in the manner described in this study.

To attack the problem of scale selection in cumulus convection, the present model is not sufficient. Additional scales of motion have to be taken into account and the most interesting aspect of this problem is to see whether it is the advective nonlinearity or the nonlinearity introduced by condensation which will determine the scale selection. In the study of Helfand and Kalnay (1983) scale selection is described in terms of open and closed cells. They specified a horizontally uniform and vertically varying heating field and thus did not take the interaction between vertical motion and condensational heating into account. The scale selection is thus only determined by the advective nonlinearity. They found that the vertical position of the heating determines the scale of motion. In a recent study by van Delden (1985) the advective nonlinearity in the vorticity equation is absent but due to the inclusion of condensation non-linear scale selection is found. It is still an open question which of these two processes is the most important one in the atmosphere, but further studies with an extended version of the model described here will be undertaken to obtain a better understanding of this problem.

6. Acknowledgments

We would like to thank Prof. Hilding Sundqvist, University of Bergen, Norway, and Prof. Bert Bolin, University of Stockholm, Sweden, for discussions and critical comments. This study was supported by NFR (Swedish National Science Research Council) contracts no. S-FO 1705-107 and G-GU 1705-106.

7. Appendix A

Derivation of the moist adiabatic lapse rate

The modified Clausius-Clapeyron equation can be written as:

$$\frac{1}{q_s} \frac{dq_s}{dt} = \frac{L_v}{R_v T^2} \frac{dT}{dt} - \frac{1}{p} \frac{dp}{dt} \tag{A.1}$$

In the moist adiabatic processes, the equivalent

potential temperature θ_e is a conservative quantity:

$$\theta_e = \theta_p \exp \left\{ \frac{L_v q_s}{c_p T} \right\}, \tag{A.2}$$

so,

$$\begin{aligned} \frac{d\theta_e}{\theta_e} &= \frac{d\theta_p}{\theta_p} + d \left(\frac{L_v q_s}{c_p T} \right) \\ &= \frac{dT}{T} \left(1 + \frac{\epsilon L_v^2 q_s}{c_p R_d T^2} \right) - \frac{R_d}{c_p} \frac{dp}{p} \left(1 + \frac{L_v q_s}{R_d T} \right) = 0, \end{aligned}$$

where θ_p is the potential temperature. Using the hydrostatic approximation, we obtain:

$$\begin{aligned} \Gamma_m &= - \left(\frac{\partial T}{\partial z} \right)_{\theta_e = \text{constant}} \\ &= \frac{pg}{R_d T} \left(\frac{\partial T}{\partial p} \right)_{\theta_e = \text{constant}} \\ &= \frac{pg}{R_d T} \frac{R_d T}{c_p p} \left(1 + \frac{L_v q_s}{R_d T} \right) / \left(1 + \frac{q L_v^2 q_s}{c_p R_d T^2} \right) \\ &= \Gamma_d \left(1 + \frac{L_v q_s}{R_d T} \right) / \left(1 + \frac{\epsilon L_v^2 q_s}{c_p R_d T^2} \right), \\ \Gamma_d - \Gamma_m &= \Gamma_d \frac{L_v q_s (\epsilon L_v - c_p T)}{c_p R_d T^2 + \epsilon L_v^2 q_s}. \end{aligned}$$

8. Appendix B

The specific humidity approximated by a height dependent function

The basic temperature distribution is:

$$T_0(z) = T_0 - \Gamma z; \tag{B.1}$$

here, T_0 is the temperature at $z = 0$, Γ is the lapse rate of temperature. The definition of saturated specific humidity q_s can be used:

$$q_s = \frac{\epsilon E_0}{P} \exp \left\{ \frac{\epsilon L_v}{R_d} \left(\frac{1}{T_0} - \frac{1}{T} \right) \right\}, \tag{B.2}$$

where P is the pressure and E_0 is the saturation vapour pressure at T_0 . Furthermore, using the hydrostatic approximation the pressure can be treated as a function of height only:

$$P = P_0 \exp \left\{ - \frac{gz}{R_d \bar{T}} \right\}, \tag{B.3}$$

where P_0 is the pressure at $z = 0$ and \bar{T} is the

mean temperature. We can now express the saturated specific humidity as a function of height:

$$\begin{aligned}
 q &= \frac{\epsilon E_0}{P_0} \exp\left\{\frac{gz}{R_d \bar{T}}\right\} \exp\left\{\frac{\epsilon L_v}{R_d} \left(\frac{1}{T_0} - \frac{1}{T_0 - \Gamma z}\right)\right\} \\
 &= q_0(0) \exp\left\{\frac{gz}{R_d \bar{T}}\right\} \exp\left\{-\frac{\epsilon L_v \Gamma z}{R_d T_0 (T_0 - \Gamma z)}\right\} \\
 &= q_0(0) \exp\left\{\left(\frac{g}{R_d \bar{T}} - \frac{\epsilon L_v \Gamma}{R_d T_0 (T_0 - \Gamma z)}\right) z\right\} \\
 &= q_0(z). \tag{B.4}
 \end{aligned}$$

9. Appendix C

Some details of deriving the low-order model

The basic equations in the non-dimensional form as in (2.9) and (2.10) are:

$$\frac{\partial \nabla^2 \Psi}{\partial t} = -\frac{\partial(\Psi, \nabla^2 \Psi)}{\partial(y, z)} + \sigma \frac{\partial \theta}{\partial y} + \sigma \nabla^4 \Psi \tag{C.1}$$

$$\begin{aligned}
 \frac{\partial \theta}{\partial t} &= -\frac{\partial(\Psi, \theta)}{\partial(y, z)} + (R + H_n \delta_1) \frac{\partial \Psi}{\partial y} \\
 &+ (1 - M_n \delta_1) \nabla^2 \theta. \tag{C.2}
 \end{aligned}$$

The streamfunction and temperature deviation are expressed by using four components as in eqs. (3.3):

$$\Psi = F(t) \sqrt{2} \sin ay \sin z \tag{C.3}$$

$$\begin{aligned}
 \theta &= A(t) \sqrt{2} \cos ay \sin z + B(t) \sin 2z \\
 &+ C(t) \sin z. \tag{C.4}
 \end{aligned}$$

Substituting (C.3) and (C.4) into (C.1) and (C.2):

$$\begin{aligned}
 &-\sqrt{2}(1+a^2) \sin ay \sin z \, dF/dt \\
 &= -\sigma \sqrt{2} a \sin ay \sin z A
 \end{aligned}$$

$$\begin{aligned}
 &\sqrt{2} \cos ay \sin z \, dA/dt + \sin 2z \, dB/dt + \sin z \, dC/dt \\
 &= -FA \sqrt{2} a \sin z \cos z - FB 2 \sqrt{2} a \cos ay \sin z \\
 &- FC \sqrt{2} a \cos ay \sin z \cos z \\
 &+ FR \sqrt{2} a \cos ay \sin z \\
 &+ F \delta_1 H_n \sqrt{2} a \cos ay \sin z \tag{1}
 \end{aligned}$$

$$\begin{aligned}
 &-A(1+a^2) \sqrt{2} \cos ay \sin z \\
 &+ A \delta_1 M_n \sqrt{2} (1+a^2) \cos ay \sin z \tag{2}
 \end{aligned}$$

$$\begin{aligned}
 &-B 4 \sin 2z + B \delta_1 M_n 4 \sin 2z - C \sin z \\
 &\tag{3}
 \end{aligned}$$

$$\begin{aligned}
 &+ C \delta_1 M_n \sin z. \tag{4} \\
 &\tag{C.6}
 \end{aligned}$$

There are four terms, marked by (1), (2), (3) and (4), come from the condensation. We only give the details connected to these terms in the course of the integrations.

From the integration

$$\int_0^{2\pi/a} \int_0^\pi (C.5)/2 \sin ay \sin z \, dy dz,$$

we get:

$$dF/dt = -\sigma(1+a^2)F + \frac{a\sigma}{1+a^2} A. \tag{C.7}$$

In the integration

$$\int_0^{2\pi/a} \int_0^\pi (C.6)/2 \cos ay \sin z \, dy dz,$$

we have:

$$(1) \, 2aF \int_0^{2\pi/a} \int_0^\pi \delta_1 H_n \cos^2 ay \sin^2 z \, dy dz$$

$$\begin{aligned}
 &= \begin{cases} 2aF \int_{-z_h}^\pi dz \left\{ \int_0^{\pi-2a} dy + \int_{3\pi-2a}^{2\pi} dy \right\} H_n \sin^2 z \cos^2 ay & F > 0 \\ 0 & F = 0 \\ 2aF \int_{-z_h}^\pi dz \int_{\pi-2a}^{3\pi-2a} dy H_n \sin^2 z \cos^2 ay & F < 0 \end{cases} \\
 &= \frac{\pi^2}{a} a \frac{H_a}{2} F,
 \end{aligned}$$

$$+\sigma \sqrt{2}(1+a^2)^2 \sin ay \sin z F, \tag{C.5} \quad \text{where}$$

$$H_a = \frac{2}{\pi} \int_{z_b}^{\pi} H_n \sin^2 z \, dz. \tag{C.8}$$

$$\begin{aligned} (2) \quad & 2(1 + a^2)A \int_0^{2\pi/a} \int_0^{\pi} \delta_1 M_n \sin^2 z \cos^2 ay \, dydz \\ &= \frac{\pi^2}{a} \frac{\sqrt{2}}{\pi} a \delta_2 H_b F, \\ &= \frac{\pi^2}{a} (1 + a^2) \frac{M_a}{2} A, \end{aligned}$$

where

$$M_a = \frac{2}{\pi} \int_{z_b}^{\pi} M_n \sin^2 z \, dz. \tag{C.9}$$

$$\begin{aligned} (3) \quad & 4\sqrt{2}B \int_0^{2\pi/a} \int_0^{\pi} \delta_1 M_n \sin z \sin 2z \cos ay \, dydz \\ &= 4\sqrt{2}B \frac{2}{a} \delta_2 \int_{z_b}^{\pi} M_n \sin z \sin 2z \, dz \\ &= \frac{\pi^2}{a^4} \frac{\sqrt{2}}{\pi} \delta_2 M_b B, \end{aligned}$$

where

$$\delta_2 = \begin{cases} -1 & F < 0 \\ 0 & F = 0. \\ +1 & F > 0 \end{cases} \tag{C.10}$$

and

$$M_b = \frac{2}{\pi} \int_{z_b}^{\pi} M_n \sin z \sin 2z \, dz. \tag{C.11}$$

$$\begin{aligned} (4) \quad & \sqrt{2}C \int_0^{2\pi/a} \int_0^{\pi} \delta_1 M_n \sin^2 z \cos ay \, dydz \\ &= \sqrt{2}C \frac{2}{a} \delta_2 \int_{z_b}^{\pi} M_n \sin^2 z \, dz = \frac{\pi^2 \sqrt{2}}{a\pi} \delta_2 M_c C. \end{aligned}$$

So we get:

$$\begin{aligned} \frac{dA}{dt} &= a(R + \frac{1}{2}H_a)F - (1 + a^2)(1 - \frac{1}{2}M_a)A \\ &+ 4 \frac{\sqrt{2}}{\pi} M_b \delta_2 B + \frac{\sqrt{2}}{\pi} \delta_2 M_c C + aFB. \end{aligned} \tag{C.12}$$

In the integration

$$\int_0^{2\pi/a} \int_0^{\pi} (C.6)/2 \sin 2z \, dydz,$$

we get:

$$(1) \quad a\sqrt{2}F \int_0^{2\pi/a} \int_0^{\pi} \delta_1 H_n \cos ay \sin z \sin 2z \, dydz$$

$$\begin{aligned} &= a\sqrt{2}F \frac{2}{a} \delta_2 \int_{z_b}^{\pi} H_n \sin z \sin 2z \, dz \\ &= \frac{\pi^2}{a} \frac{\sqrt{2}}{\pi} a \delta_2 H_b F, \end{aligned} \tag{C.13}$$

where

$$H_b = \frac{2}{\pi} \int_{z_b}^{\pi} H_n \sin z \sin 2z \, dz. \tag{C.13}$$

$$\begin{aligned} (2) \quad & \sqrt{2}(1 + a^2)A \int_0^{2\pi/a} \int_0^{\pi} \delta_1 M_n \\ & \times \cos ay \sin z \sin 2z \, dydz \\ &= \sqrt{2}(1 + a^2)A \frac{2}{a} \delta_2 \int_{z_b}^{\pi} M_n \sin z \sin 2z \, dydz \\ &= \frac{\pi^2}{a} \frac{\sqrt{2}}{\pi} (1 + a^2) \delta_2 M_b A. \end{aligned}$$

$$\begin{aligned} (3) \quad & 4B \int_0^{2\pi/a} \int_0^{\pi} \delta_1 M_n \sin^2 2z \, dydz \\ &= 4B \frac{\pi}{a} \int_{z_b}^{\pi} M_n \sin^2 2z \, dz = \frac{\pi^2}{a} 2M_c B, \end{aligned}$$

where

$$M_c = \frac{2}{\pi} \int_{z_b}^{\pi} M_n \sin^2 2z \, dz. \tag{C.14}$$

$$\begin{aligned} (4) \quad & C \int_0^{2\pi/a} \int_0^{\pi} \delta_1 M_n \sin z \sin 2z \, dydz \\ &= C \frac{\pi}{a} \int_{z_b}^{\pi} M_n \sin z \sin 2z \, dz = \frac{\pi^2}{a} \frac{1}{2} M_b C. \end{aligned}$$

So, we get

$$\begin{aligned} \frac{dB}{dt} &= a \frac{\sqrt{2}}{\pi} H_b \delta_2 F + \frac{\sqrt{2}}{\pi} (1 + a^2) M_b \delta_2 A \\ &- 4(1 - \frac{1}{2}M_c)B + \frac{1}{2}M_b C - aFA. \end{aligned} \tag{C.15}$$

In the integration

$$\int_0^{2\pi/a} \int_0^{\pi} (C.6)/2 \sin z \, dydz,$$

we get:

$$\begin{aligned} (1) \quad & a\sqrt{2}F \int_0^{2\pi/a} \int_0^{\pi} \delta_1 H_n \cos ay \sin^2 z \, dydz \\ &= a\sqrt{2}F \frac{2}{a} \delta_2 \int_{z_b}^{\pi} H_n \sin^2 z \, dz \\ &= \frac{\pi^2}{a} \frac{\sqrt{2}}{\pi} a \delta_2 H_a F. \end{aligned}$$

$$\begin{aligned}
 (2) \quad & \sqrt{2}(1+a^2)A \int_0^{2\pi/a} \int_0^\pi \delta_1 M_n \cos ay \sin^2 z \, dydz \\
 &= \sqrt{2}(1+a^2)A \frac{2}{a} \delta_2 \int_{z_b}^\pi M_n \sin^2 z \, dz \\
 &= \frac{\pi^2}{a} \frac{\sqrt{2}}{\pi} (1+a^2) \delta_2 M_a A.
 \end{aligned}$$

$$\begin{aligned}
 (3) \quad & 4B \int_0^{2\pi/a} \int_0^\pi \delta_1 M_n \sin z \sin 2z \, dydz \\
 &= 4B \frac{\pi}{a} \int_{z_b}^\pi M_n \sin z \sin 2z \, dz = \frac{\pi^2}{a} 2M_b B.
 \end{aligned}$$

$$(4) \quad C \int_0^{2\pi/a} \int_0^\pi \delta_1 M_n \sin^2 z \, dydz$$

$$= C \frac{\pi}{a} \int_{z_b}^\pi M_n \sin^2 z \, dz = \frac{\pi^2}{a} \frac{1}{2} M_a C.$$

So, we get:

$$\begin{aligned}
 \frac{dC}{dt} = & a \frac{\sqrt{2}}{\pi} H_a \delta_2 F + \sqrt{2}(1+a^2) \frac{1}{\pi} M_a \delta_2 A \\
 & + 2M_b B - (1 - \frac{1}{2} M_a) C. \tag{C.16}
 \end{aligned}$$

Up to now, we have got (C.7), (C.12), (C.15) and (C.16) as the equations of our low-order model. The expressions (C.8), (C.9), (C.11), (C.13) and (C.14) give the definitions of the numbers H_a , H_b , M_a , M_b and M_c introduced by the condensation.

REFERENCES

- Asai, T. and Nakasugi, I. 1982. A further study of the preferred mode of cumulus convection in a conditionally unstable atmosphere. *J. Meteorol. Soc. Japan* 60, 425–431.
- Atkinson, B. W. 1981. *Mesoscale atmospheric circulations*. Academic Press, 487 pp.
- Haltiner, G. J. and Williams, R. T. 1980. *Numerical prediction and dynamic meteorology*. John Wiley and Sons, New York, 2nd ed., 477 pp.
- Helfand, H. M. and Kalnay, E. 1983. A model to determine open or closed cellular convection. *J. Atmos. Sci.* 40, 631–650.
- Krishnamurti, R. 1968a. Finite amplitude convection with changing mean temperature. Part 1. Theory. *J. Fluid. Mech.* 33, 445–455.
- Krishnamurti, R. 1968b. Finite amplitude convection with changing mean temperature. Part 2. An experimental test of the theory. *J. Fluid. Mech.* 33, 457–463.
- Krishnamurti, R. 1975a. On cellular cloud patterns. Part 1. Mathematical model. *J. Atmos. Sci.* 32, 1353–1363.
- Krishnamurti, R. 1975b. On cellular cloud patterns. Part 3. Applicability of mathematical and laboratory models. *J. Atmos. Sci.* 32, 1373–1383.
- Lorenz, E. N. 1963. Deterministic nonperiodic flow. *J. Atmos. Sci.* 20, 130–141.
- Saltzman, B. 1962. Finite amplitude free convection as an initial value problem—I. *J. Atmos. Sci.* 19, 329–341.
- Shirer, H. N. and Dutton, J. A. 1979. The branching hierarchy of multiple solutions in a model of moist convection. *J. Atmos. Sci.* 36, 1705–1721.
- van Delden, A. 1984. Scale selection in low-order spectral models of two-dimensional thermal convection. *Tellus* 36A, 458–479.
- van Delden, A. 1985. On the preferred mode of cumulus convection. *Beitr. Phys. Atmos.* 58, 202–219.
- van Delden, A. and Oerlemans, J. 1982. Grouping of clouds in a numerical cumulus convection model. *Beitr. Phys. Atmos.* 56, 239–252.